Anderson localization and solitonic energy transport in one-dimensional oscillatory systems

G. S. Zavt,* M. Wagner, and A. Lütze
Institut für Theoretische Physik III, Universität Stuttgart, Pfaffenwaldring 57, 7000 Stuttgart 80, Germany
(Received 29 December 1992)

In a harmonically disordered chain with a regular array of quartic nearest-neighbor anharmonicity we have found a constructive or conflicting interplay of Anderson localization and solitary solutions depending on the type of initial excitation (momentum or displacement). In the present work we specifically discuss energy propagation ensuing after the momentum excitation of a single mass. A coexistence of Anderson localization and superdiffusive energy transport is found. Further, it is found that disorder destabilizes the supersonic solitary solution, whereas conversely anharmonicity reduces Anderson localization. A detailed analysis is given.

PACS number(s): 05.60.+w, 66.70.+f

I. INTRODUCTION

The present paper addresses the problem of the combined effect of disorder and nonlinearity on the energy transport in a mechanical system of coupled anharmonic oscillators arranged in a one-dimensional lattice. Setting by initial conditions the energy at time $t=0$ to be restricted to a microscopically small region (actually, to one atom) we follow by computer simulation technique the spatiotemporal evolution of the energy density and related quantities. This problem is relevant for the theory of heat conduction in disordered systems, for the theory of relaxation processes accompanying fast energy release in a localized region (optical transitions, Mössbauer effect, nuclear transformations, photosynthesis, etc.). Disorder and anharmonicity are two main mechanisms of phonon scattering in solids. Within the conventional perturbation approach (i.e., in a weak scattering limit) these two mechanisms are considered usually as additive contributions to the scattering rate. However, in one or two dimensions such an approach seems to be basically inconsistent even for weak disorder. As is well known, an arbitrary small disorder in one or two dimensions leads to the localization of almost all eigenstates of the underlying linear system (Anderson localization [1], extended to the phonon problem in [2,3]). More precisely, for almost all random realizations of mass and/or force constant distributions, each normal mode is exponentially localized around a particular lattice site and the spectrum of normal modes is purely pointlike [2]. According to Anderson [1], the localization of wave functions (or eigenmodes) can be conceived as the absence of energy transport in a disordered system. In other words, for spatially bounded initial conditions, the diffusion coefficient (defined below) asymptotically tends to zero in the limit $t\to\infty$. Consequently, the role played by nonlinearity changes drastically: one may expect that it provides the only mechanism of energy transport rather than an additional resistive channel. This is the idea on which a recent treatment of thermal conductivity of glasses beyond the "plateau" regime has been based [4]. In an earlier paper, similar conclusions were drawn from computer experiments on heat propagation in one-dimensional (1D) systems [5].

It should be pointed out that, even for harmonic disordered systems, the relation between the localization and the absence of diffusion is not straightforward. It is known [6], that for small frequencies ω the localization length behaves as ω^{-2}, therefore, at least $\sim\sqrt{N}$ (where N is the number of atoms) low-frequency acoustical modes have a localization length of the order of the chain length. Since the fraction of such modes is of zero measure at $N\to\infty$, it is believed that their influence on physical properties is negligible. Nevertheless, it appears [6] that the energy flux connected with unscattered modes can be either infinite or zero, depending on boundary conditions. Below we reexamine this problem in an approach which is independent of boundary conditions to show that when the initial energy is projected to all modes, localization and a special kind of energy transport, called superdiffusion, are coexistent.

The essential property of 1D nonlinear dynamical systems is that most of the commonly used interatomic potential models (polynomial, Toda, Morse, Lennard-Jones) permit kink-soliton solutions (see, e.g., [7,8]). The solitonic effect causes the small-amplitude oscillations to be overtaken by the large-amplitude oscillations, which appear to be much more robust against the disorder-conditioned scattering [9]. We will demonstrate that the creation of solitons and their scattering by disorder manifests itself in three ways: (1) reduction of the amount of energy confined within the localization region; (2) acceleration of the energy transport at small times and acceleration or deceleration, depending on the nonlinearity, at large times; and (3) change of the asymptotic properties of the time-dependent diffusion coefficient. The latter point is especially essential in the context of the ergodic behavior of dynamical Hamiltonian systems.

II. THE MODEL

We consider a 1D system with nearest-neighbor interaction described by the classical Hamilton function

 ©1993 The American Physical Society

$$H=\sum_{m=-N}^{N}\left\{\frac{p_m^2}{2M_m}+\frac{f_2(m_1m+1)}{2}(q_m-q_{m+1})^2+\frac{f_4}{4}(q_m-q_{m+1})^4\right\}, \quad (1)$$

where q_m and p_m are the displacement and momentum of the mth atom. We assume there is no disorder in the anharmonic terms. Let $f\equiv f_2(m,m+1)$ and M, respectively, denote the force constant and the mass in an ideal reference harmonic chain; its maximal phonon frequency is given by $\Omega_D=2\sqrt{f/M}$. Let A be a characteristic scale for the displacement amplitude. Introducing dimensionless variables

$$\tau=\Omega_D t,\quad Q_m=q_m/A,\quad P_m=p_m/(M\Omega_D A) \quad (2)$$

and parameters

$$\mu_m=M_m/M,\quad \Phi_{mm'}=f_2(mm')/f,\quad \gamma_4=f_4A^2/f\ , \quad (3)$$

one obtains the Hamiltonian equations of motion as

$$\frac{d}{d\tau}Q_m=P_m/\mu_m\ ,$$
$$\frac{d}{d\tau}P_m=\tfrac{1}{4}\{\Phi_{m,m+1}(Q_{m+1}-Q_m)+\Phi_{m,m-1}(Q_{m-1}-Q_m)+\gamma_4[(Q_{m+1}-Q_m)^3+(Q_{m-1}-Q_m)^3]\}\ . \quad (4)$$

Thus the nonlinearity parameter γ_4 characterizes both the effects of the anharmonicity of the potential energy function and the amplitude of the vibrations. Since the total energy defined by initial conditions is proportional to A^2 one can visualize the variation of γ_4 (for a fixed potential) as the variation of the total energy. To have some idea about realistic values of γ_4 one can consider a typical potential with attraction core $V(r)\sim r^{-n}$ (e.g., Lennard-Jones, etc.). This yields $\gamma_4=(n+2)(n+3)A^2/6a^2$, where a is the lattice constant. Since typical values of n lie in the interval 9–12, the value $\gamma_4=1$ corresponds to $A\sim 0.2a$, which is close to the Lindemann criterion of melting. However, A is introduced above only as a scale; the actual values of displacements (more strictly, the difference of displacements) depend on initial conditions and normally (at least, for simulations described below) do not exceed $0.4a$; it means that even values $\gamma_4\sim 10$ may be physically reasonable.

The disorder is simulated as the variation of the force constants only, namely, we take $\Phi_{m,m+1}=f'/f$ with probability c or $\Phi_{m,m+1}=1$ with probability $1-c$. While for the harmonic chain force constant and mass disorder are equivalent, this no longer holds for the nonlinear case.

Except for the disorder, Hamiltonian (1) corresponds to the famous Fermi-Pasta-Ulam (FPU) β problem [10]. FPU used as initial conditions the exact eigenmodes of the harmonic system and studied the energy redistribution between the modes, which led them to the discovery of the excitation recurrence phenomena explained later as the manifestation of solitons [11]. Our goal is, however, to study the evolution of originally localized excitations, i.e., those which project onto all lattice modes. Therefore we choose the initial conditions (below denoted as P type) as

$$P_m(0)=\delta_{m0},\quad Q_m(0)=0\ \text{ for all } m\ . \quad (5)$$

The spatial and temporal evolution of the energy of lattice vibrations, originally localized at the center $m=0$ of the lattice, will be described by the energy density (in units $M\Omega_D^2A^2$)

$$h_m(\tau)=\frac{P_m^2(\tau)}{2\mu_m}+\sum_{m'=m\pm1}\left\{\frac{\Phi_{mm'}}{16}[Q_m(\tau)-Q_{m'}(\tau)]^2+\frac{\gamma_4}{32}[Q_m(\tau)-Q_{m'}(\tau)]^4\right\}, \quad (6)$$

while the spreading of the energy distribution is measured by its second moment

$$M_2(\tau)=\sum_m |m|^2h_m(\tau)\ . \quad (7)$$

Then the diffusion coefficient is defined as

$$D=\lim_{\tau\to\infty}D(\tau)\equiv\lim_{\tau\to\infty}M_2(\tau)/(M_0\tau)\ , \quad (8)$$

where $M_0=\sum_m h_m(\tau)$ is the total energy. This quantity is analogous to the diffusion coefficient introduced by Anderson [1] and studied in similar context, e.g., in [12,13]. Assuming $D(\tau)\sim\tau^\alpha$ at $\tau\to\infty$ we can describe the main regimes of the energy evolution as follows: $\alpha=1$, $\alpha=0$, and $\alpha<0$, respectively, denote coherent (ballistic) energy transport, usual diffusion, and localization. The fractional values of α or nonalgebraic behavior of $D(\tau)$ are usually referred to as an anomalous diffusion.

We solve numerically Eqs. (4) with initial condition (5) by fourth-order predictor-corrector method. The chain is treated in a self-expanding manner [14], i.e., we start with a short chain and expand it as the energy on the last atoms approaches the preset small value. This approach is based on the observation that, although Eqs. (4) do not include the retardation effects, the displacements of atoms beyond the propagating front are exponentially small. In this sense, for every given time, the chain is effectively infinite, i.e., the influence of boundaries, reflection processes, etc. is excluded.

The meaning of the long-time limit is crucial for the present problem. Its usual definition is $\tau\to\infty$ while the number of particles is large but finite (see, e.g., [15] and references therein). Since the system is conservative and nonintegrable one cannot expect any simple asymptotic behavior—instead, the system evolves to complicated Poincaré cycles which arise due to the reflections from the end atoms. Within the Poincaré cycle the behavior of a system is quasiergodic in the sense that the fluctuations of the energy density are of the order $1/N$. The asymptotics considered here means τ is large but $\tau<N$, i.e., this corresponds to the "first passage" of the energy. Physically, such a limit is more adequate for the problems involving energy transport, e.g., the heat conductivity.

III. BACKGROUND AND OVERVIEW

One of the main stimuli for the present calculation was the recent theoretical manifestation of unexpected features for the energy propagation in one of the most simple physical systems, which is the "Hamiltonian chain" (harmonic nearest-neighbor interaction [16]). It turned out that the spatial energy evolution displays a pronounced dependence on the nature of the initial localized excitation. If the excitation is of momentum type ("P type"), as specified in (5), the energy $h_m(\tau)$ pertaining to cell m at time $\tau=\Omega_D t$ is given by (see [17])

$$h_m(\tau)=\tfrac{1}{2}[J^2_{2|m|}(\tau)+\tfrac{1}{2}J^2_{2|m|+1}(\tau)+\tfrac{1}{2}J^2_{2|m|-1}(\tau)] \ . \tag{9}$$

The spatial distribution of $h_m(\tau)$ for a given instant is shown in Fig. 1. One recognizes on the one hand a plateau region around the initial excitation site $m=0$, and on the other hand the appearance of sharp peaks at the sound-velocity boundaries $m=\pm\tau/2$, the sound velocity (in dimensionless units) given by $v=\frac{1}{2}$. The intensity at the wind maxima behaves like $\tau^{-2/3}$ while behind the front ($|m|\ll\tau/2$) it drops like τ^{-1}, making the trailing edge of the front more steep in the course of the evolution; however, the dispersive oscillatory regime between the wing peaks persists for all times (see Fig. 1).

A contrast to this behavior is established by the energy propagation following a displacement type "(Q type") of initial condition:

$$P_m(0)=0 \ \text{ for all } m, \quad Q_m(0)=\delta_{m0} \ . \tag{10}$$

In this case the energy $h_m(\tau)$ pertaining to all m at time $\tau=\Omega_D t$ is given by (see [17])

$$h_m(\tau)=\frac{1}{4}\left[2\left[\frac{d}{d\tau}J_{2|m|}(\tau)\right]^2+\left[\frac{d}{d\tau}J_{2|m|+1}(\tau)\right]^2+\left[\frac{d}{d\tau}J_{2|m|-1}(\tau)\right]^2\right] \tag{11}$$

and for a given instant this behavior is depicted in Fig. 2. One notices that now wing maxima at the sound-velocity edges $|m|=\tau/2$ do not appear and that the maximum of the distribution remains in the central region around $m=0$. A global characterization of this contrasting behavior can be given by the relative second moment, which for P excitation is found to be [17]

$$[M_2(\tau)/M_0]^{(P)}=\frac{1}{2}\left[\frac{\tau}{2}\right]^2 \tag{12}$$

whereas for Q excitation [17] we have

$$[M_2(\tau)/M_0]^{(Q)}=\frac{1}{4}\left[\frac{\tau}{2}\right]^2 \ . \tag{13}$$

Thus in a rough qualitative characterization one may state that *momentum excitation is more favorable to energy propagation than displacement excitation.*

One of the main aims of our present work is to find out whether these contrasting features prevail, if disorder or anharmonicity or both are brought into the system. In this paper we specifically will turn our attention to the

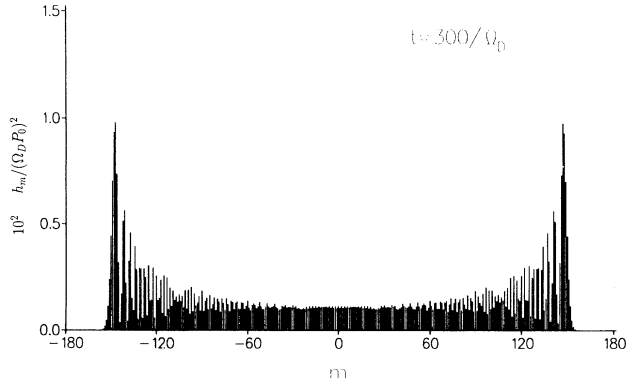

FIG. 1. Spatial evolution of the energy $h_m(\tau)$ per site m in the Hamiltonian chain [17]. Time $\tau=300$. Initial ($\tau=0$) momentum excitation P_0 at site $m=0$.

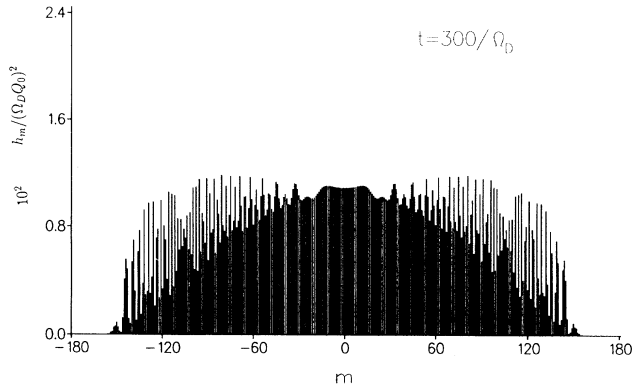

FIG. 2. Spatial evolution of the site energy h_m per site m in the Hamiltonian chain. Time $\tau=300$. Initial ($\tau=0$) displacement excitation Q_0 at site $m=0$.

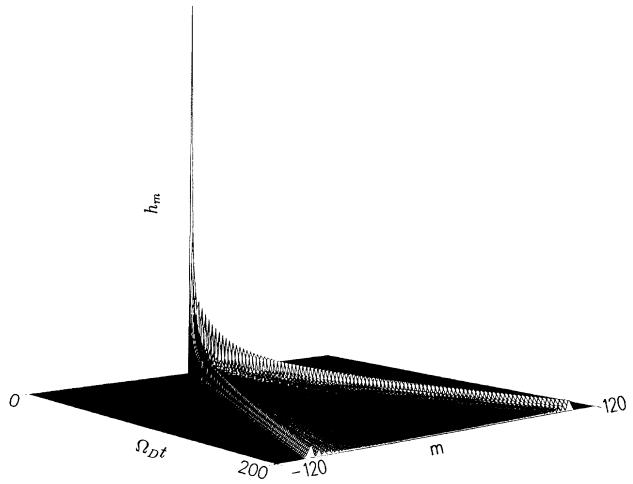

FIG. 3. Spatiotemporal evolution of the site energy $h_m(\tau)$ in the ideal harmonic chain (nearest-neighbor interaction). Initial ($\tau=0$) momentum excitation at site $m=0$.

momentum excitation case as defined by (5). An overview of our findings is visualized in Figs. 3–6. Figure 3 shows the spatiotemporal display of the site energy $h_m(\tau)$ in the Hamiltonian chain (equal nearest-neighbor springs, equal masses) after P excitation at site $m=0$.

If harmonic disorder is introduced by replacing a portion of regular springs f by a second type f' (concentration c) in a random manner, the energy density separates in a rather short time after the excitation in two components: a nonpropagating one, localized around the excitation site [1], and two decaying comparatively sharp maxima moving in opposite directions. This is shown in Fig. 4.

If, on the other hand, the chain remains regular, but a quartic nearest-neighbor spring f_4 in addition to the harmonic one ($f_2=f$) is introduced, the wing peaks of Fig. 3 (see also Fig. 1) beyond a certain excitation strength are transmuted into stable solitons, which separate from the sound-velocity edge. This is shown in Fig. 5.

Finally, if both anharmonicity and disorder are present, both wing solitons and Anderson localization simultaneously appear in the evolutionary process. But on the one hand the wing solitons are no longer stable, whereas on the other hand anharmonicity has the effect of reducing the energy portion which is captured in a given region around $m=0$. This is shown in Fig. 6.

Thus in a rough qualitative manner one may characterize the energy propagation which ensues after a momentum excitation by the following features (P case).

(A) Regular anharmonicity enforces energy propagation (ultrasonic soliton).

(B) Disorder diminishes energy propagation (Anderson localization).

(C) Disorder (harmonic) and anharmonicity (regular) counteract each other: anharmonicity reduces localization, whereas disorder destroys solitonic stability.

In the remainder of this work we will describe and discuss these features in more detail and postpone the analysis of the contrasting Q-excitation case to a forthcoming paper. For completeness, however, we mention the dominant features of the energy propagation in the Q-excitation case.

(A) Anharmonicity reduces energy propagation (localized soliton of oscillating type [18,19]).

(B) Disorder also diminishes energy propagation (Anderson localization).

(C) Disorder and anharmonicity have the same tendency with respect to transport, and accordingly disorder does not destabilize the localized solitary solution.

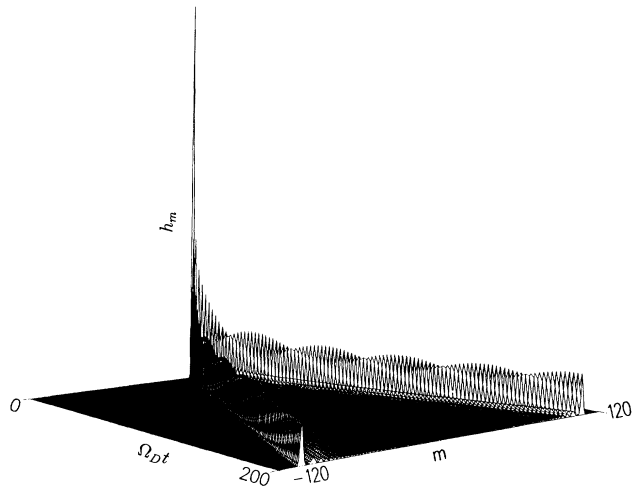

FIG. 5. Spatiotemporal evolution of the site energy $h_m(\tau)$ in the ideal anharmonic chain ($\gamma_4=1$, nearest-neighbor harmonic and quartic interaction). Initial ($\tau=0$) momentum excitation at site $m=0$.

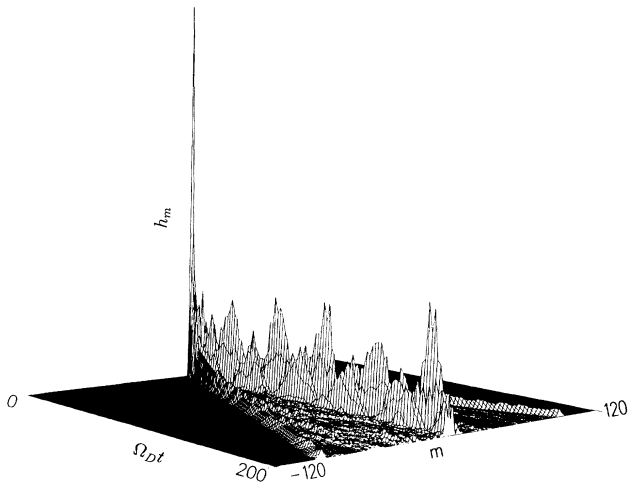

FIG. 4. Spatiotemporal evolution of the site energy $h_m(\tau)$ in the disordered harmonic chain ($c=0.2$, $f'/f=0.5$). Initial ($\tau=0$) momentum excitation at $m=0$.

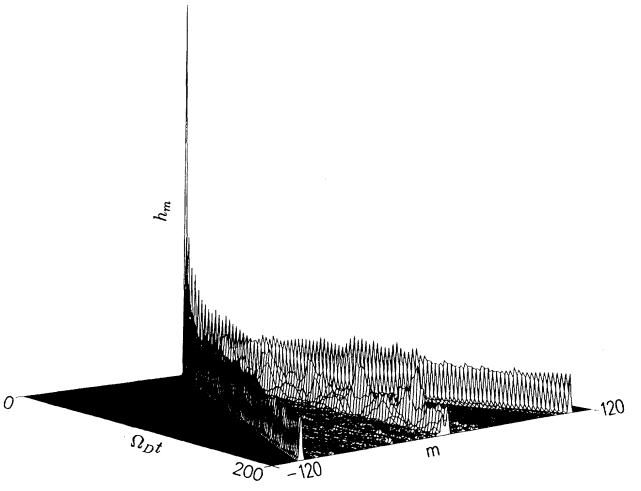

FIG. 6. Spatiotemporal evolution of the site energy $h_m(\tau)$ in the disordered anharmonic chain (harmonic nearest-neighbor spring disorder, regular quartic anharmonicity, $c=0.2$, $f'/f=0.5$, $\gamma_4=1$). Initial ($\tau=0$) momentum excitation at site $m=0$.

IV. ORDERED LATTICE: SOLITONS AND COHERENT TRANSPORT

According to usual textbook treatment of anharmonic effects one can expect the characteristic features of the harmonic picture to be smoothed out, when nonlinear terms are included. In a one-dimensional system, however, the situation is just the opposite: the energy of the conventional normal modes is overtaken by large-amplitude supersonic excitations which propagate without any losses across the lattice. These excitations represent compression kinks in the Q picture, or solitons in the P or energy picture. Analytically, these particular solutions of the equation of motion (4) are an outgrowth of the exponential solutions $\exp[\pm(\mu n-\lambda\tau)]$ pertaining to the harmonic part of Eq. (4). By means of the anharmonicity the ascending and descending exponentials establish the wings of the soliton. In this manner the latter may be written as an odd function of $u=\mathrm{sech}(\mu n-\lambda\tau)$ and satisfies the ultrasound condition

$$v_{\mathrm{sol}}=\frac{\lambda}{\mu}=\frac{1}{\mu}\sinh\left[\frac{\mu}{2}\right]=v\left(1+\tfrac{1}{24}\mu^2+\cdots\right), \qquad (14)$$

which for $\mu\to 0$ merges into the dimensionless sound velocity $v=\frac{1}{2}$. μ is a parameter which characterizes the solitonic amplitude.

Theoretical literature on solitons in continuous media is vast. A good reference is the book of Trullinger, Zakharov, and Pokrovsky [20] and the enlightening review of Bishop, Krumhansl, and Trullinger [21]. In our context in the continuum limit, i.e., under the assumption of a large width of the soliton as compared to the lattice constant, Eq. (4) transforms to the modified Korteweg–de Vries (KdV) equation which has analytical soliton solutions [22]. For reference purposes it is quite beneficial to note the Wadati solution of the modified KdV equation, which pertains to our basic set of equations of motion (4) [22]:

$$P_n(\tau)=\frac{\mu}{(24\gamma_4)^{1/2}}\frac{1}{\cosh[\mu n-\tau\sinh(\mu/2)]}, \qquad (15)$$

where μ depends on the "amplitude-nonlinearity" parameter γ_4, $\mu=\mu(\gamma_4)$.

In a discrete lattice the functional form (15) is a good approximation only for $\mu\ll 1$, although $P_n(\tau)$ remains a function of the propagation variable $[\mu n-\tau\sinh(\mu/2)]$. This easily may be shown analytically by means of a "wing expansion" of the solitary solution. The solitons in a discrete lattice for Hamilton function (1) were studied to some extent, e.g., in [23] and more recently in [24], however, a more complete knowledge about their properties remains desirable. Below we briefly list the main conclusions from our simulations, leaving a more detailed presentation for a separate publication. Figure 7 demonstrates the process of soliton creation. Increasing the nonlinearity parameter γ_4 in the interval $[0,\simeq 0.6]$ the maximum at the propagating front becomes steeper and moves slightly faster. With a further increase of the nonlinearity (or the total energy) a sharp excitation separates from the front and moves with a constant supersonic ve-

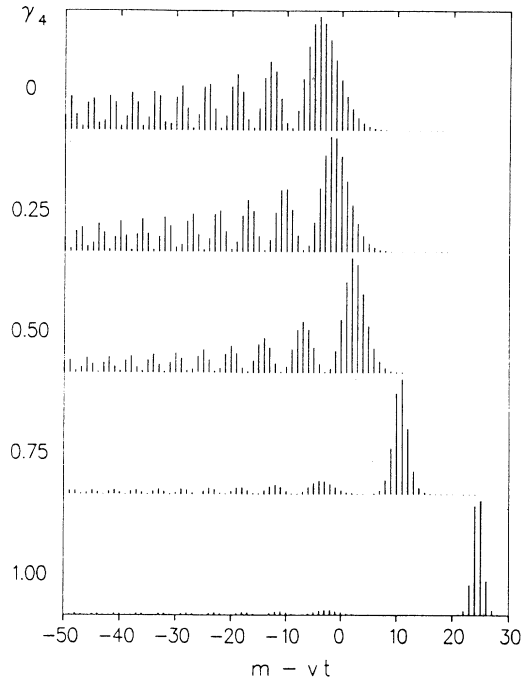

FIG. 7. Generation of a soliton above the sound-velocity edge. The amplitude is the energy $h_m(\tau)$ per lattice site m. Time $\tau=1000$. Initial ($\tau=0$) momentum excitation at site $m=0$ in the ideal anharmonic chain.

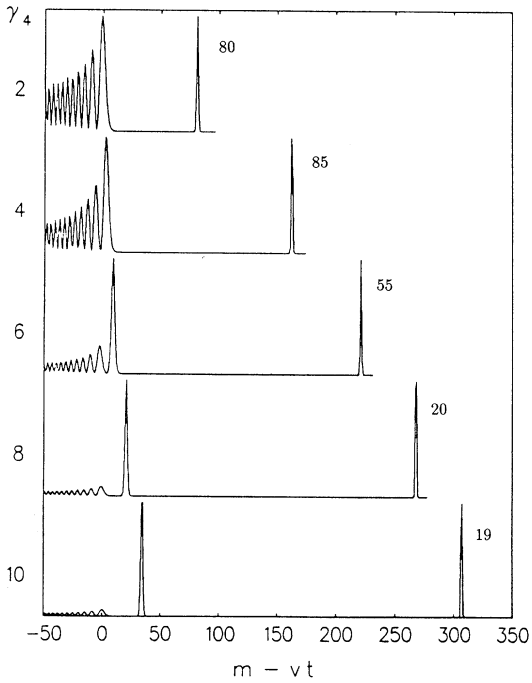

FIG. 8. Generation of a compressive soliton followed by a rarefactive one. The amplitude is the energy $h_m(\tau)$ per lattice site m. γ_4: anharmonicity parameter (see text). Time $\tau=1000$. The numbers at the upper solitonic peaks indicate multiplication factors with respect to the rest of the figure. Initial ($\tau=0$) momentum excitation at site $m=0$, ideal anharmonic chain.

locity. The soliton width decreases very fast with nonlinearity and for $\gamma_4 \simeq 1.5$ the half width at half maximum (HWHM) becomes less than one lattice constant. The amplitude $P_m(\tau)$ behaves linearly with γ_4 for weak nonlinearity and as $\gamma_4^{1/2}$ for strong nonlinearity. The soliton velocity grows linearly both for small and large γ_4, however, the slope is larger for strong nonlinearity; in the last case the velocity approaches quadratic dependence upon the amplitude.

Thus the properties of solitons are rather different depending on the strength of the nonlinearity, the demarcation line being the value $\gamma_4 \sim 1.5$ when HWHM of the soliton drops to the lattice constant. In addition, at $\gamma_4 \simeq 4.8$ a new, rarefactive, soliton moving much slower than the compressive one, is created (Fig. 8). In the limit of a pure anharmonic lattice [i.e., with $f_2 \equiv 0$ in (1)] an infinite number of solitons (alternatively compressive and rarefactive) exists; their velocities v_S are related as $1:1/\sqrt{2}:1\sqrt{6}:\cdots$, and the amplitudes are proportional to v_S^2.

The soliton shape is invariant only with respect to the discrete time translations $\Delta\tau_n = n/v_S$ where n is an integer and v_S is the soliton velocity. The change of the soliton shape when it moves between two neighboring sites is shown in Fig. 9 in the momentum, coordinate, and energy representations.

In the context of energy propagation the essential property of a nonlinear system is the suppression of dispersive decay of a propagating pulse. Figure 10

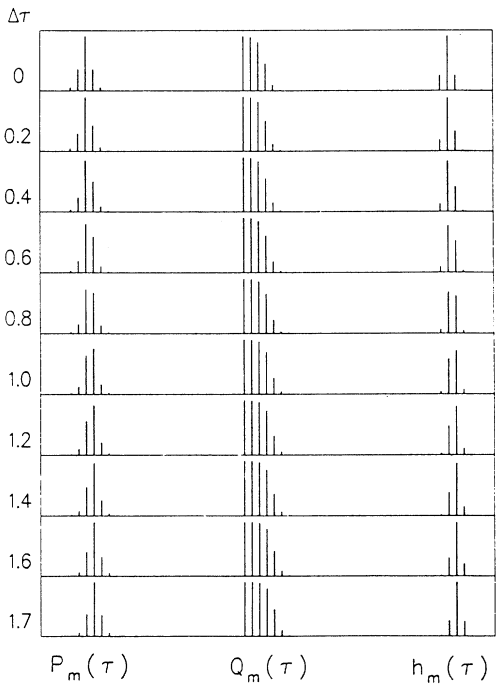

FIG. 9. Change of the solitonic shape, when the center moves from one lattice site to the next one. Anharmonicity parameter $\gamma_4 = 2$. Initial ($\tau = 0$) momentum excitation at site $m = 0$ in the ideal anharmonic chain.

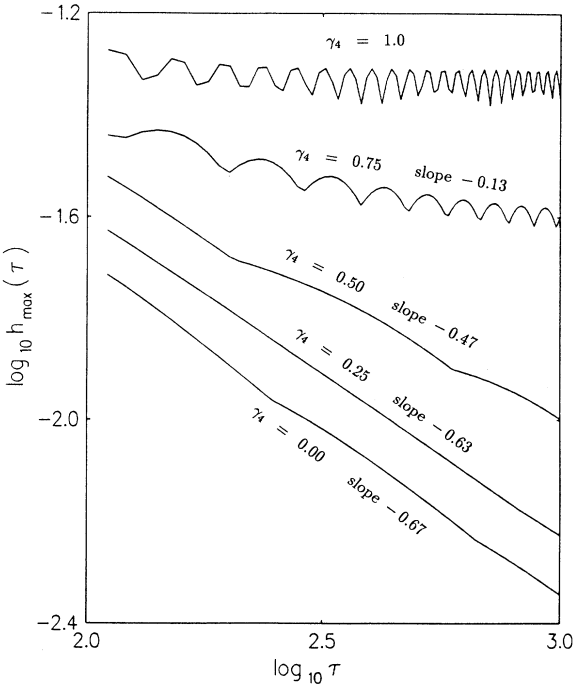

FIG. 10. Decay of the peak at the sound-velocity edge, $h_{\max}(\tau) \sim \tau^s$. s: slope as indicated. γ_4 is the anharmonicity parameter. Initial ($\tau = 0$) momentum excitation at site $m = 0$ in the ideal anharmonic chain.

demonstrates the change of the decay exponent for the main energy density maximum. For the linear lattice we obtain $\tau^{-2/3}$ law in accordance with (9); with increasing nonlinearity the exponent starts to decrease ending with zero value at $\gamma_4 \simeq 0.8$. The nondecaying soliton modes store a considerable amount of the total energy—from 0.44 at $\gamma_4 = 1$ to 0.75 at $\gamma_4 = 10$.

The diffusion coefficient turns out for all values of γ_4 to grow (asymptotically) linearly with time, the prefactor being proportional to the energy stored in the soliton modes (Fig. 11). While such behavior for the prefactor is obvious for the soliton contribution it is not evident for

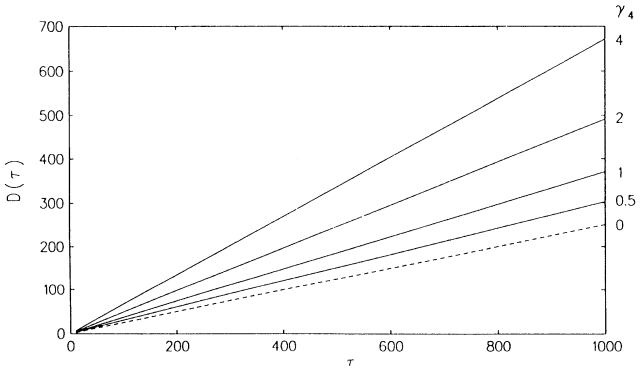

FIG. 11. Diffusion function $D(\tau) = M_2(\tau)/M_0\tau$ for the regular chain with nearest-neighbor harmonic and quartic springs. P-type excitation at site $m = 0$ at $\tau = 0$. γ_4 is the anharmonicity parameter (see text).

the residual contribution, which is not small especially for weak and moderate nonlinearity. We found a similar linear behavior of the diffusion function for 2D lattices as well, which demonstrates the universal nature of the coherent transport for ordered systems.

This allows for an illuminating view of the ergodicity problem. In the famous numerical experiment of Fermi, Pasta, and Ulam [10] it was proved for the first time that a weak nonlinearity is not sufficient to lead a Hamiltonian system to equipartition of the energy among the normal modes, neither is it sufficient to fully destroy the phase correlations between the modes. Both phenomena are considered a prerequisite of stochasticity. In a later work numerical simulations of finite systems seem to show the existence of a stochasticity threshold at a fixed value of the nonlinear coupling constant. In particular, after excitation of a group of modes [25] an equipartition threshold indicative of random phases is found for a rather low "averaged nonlinearity" ($\gamma_4 \approx 0.1$). By contrast, in our uniform infinite system the initial excitation in point of fact already amounts to an equipartition of the energy between the (harmonic) normal modes $[h(k,t=0) = M\Omega_D^2 A^2/2(2N+1)]$, but phase randomization is never achieved and even in the strong nonlinearity situation the transport remains *nondiffusive* ($D \sim t$).

V. HARMONIC DISORDERED LATTICE: LOCALIZATION AND SUPERDIFFUSION

As is evident from Fig. 4, the energy density separates in a rather short time after the excitation into two components: a nonpropagating one, localized around the excitation site, and two decaying comparatively sharp maxima moving in opposite directions.

The energy distribution in the localized part is defined by the projection of the initial excitation on the modes localized near the origin and, therefore, depends on a particular distribution of force constants. Increasing the disorder by changing the concentration or the ratio f'/f the size of the localization domain diminishes while the amount of energy stored in this region increases (Fig. 12). We describe the localization by introducing a "regional" (restricted) 0th moment

$$M_0(L,\tau) = \sum_{m=-L}^{L} h_m(\tau) \ . \tag{16}$$

For any given sufficiently strong disorder one can find such L that the amount of energy confined within the interval $(-L,L)$ remains essentially constant (Fig. 13). The value of L found in such a way gives an averaged (and rather crude) estimation of the localization length. It should be noted that in a strongly disordered system more than 90% of the initial energy remains localized within the interval of the order of 50 lattice constants.

The energy transport is determined by the part of the energy leaving the excitation region. This part, caused by weakly scattered phonons, turns out to be quite interesting. First, we notice that it is headed by a distinct maximum moving with a constant velocity close to renormalized sound velocity $v^* = v\sqrt{\langle f \rangle / f}$ where $\langle\ \rangle$ means the average over the distribution of force constants; in our case $\langle f \rangle = cf' + (1-c)f$. Second, the shape of the energy distribution within the propagating edge region can approximately be described as a Gaussian one. Both the velocity and energy distribution are subjected to fluctuations caused by the scattering events. These points are demonstrated in Fig. 14, where the heading structure of the propagating front is shown in a reference frame moving with velocity slightly smaller than v^*. The energy density at the maximum decays as τ^{-1} while the width increases proportional to $\tau^{1/2}$, so the energy stored by weakly scattered phonons decays as $\tau^{-1/2}$.

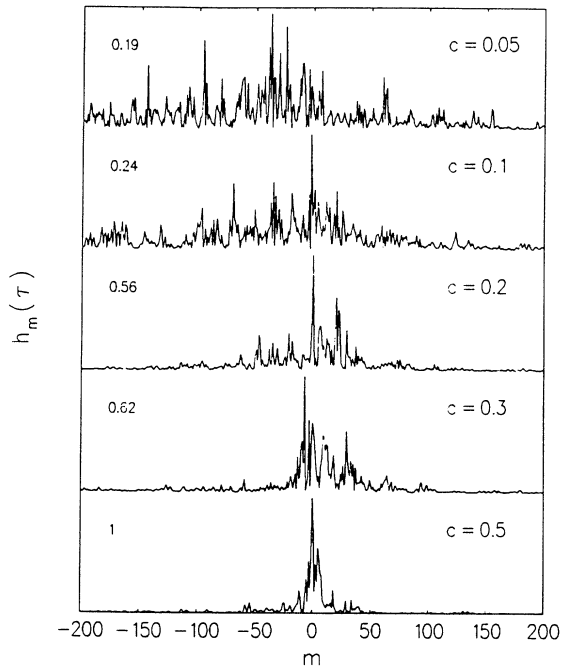

FIG. 12. Anderson localization after initial ($\tau=0$) momentum excitation at site $m=0$. Concentration $c=0.2$ of randomly distributed springs $f'/f=0.5$. Arbitrary units for $h_m(\tau)$. The numbers on the left indicate the change of the scale.

The time-dependent energy distribution among the lo-

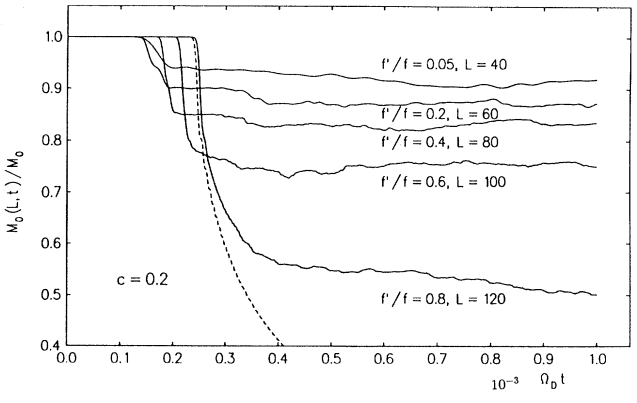

FIG. 13. Energy localization (in the disordered harmonic chain) between $m=\pm L$ (L is the localization length). c: concentration of disturbed springs. Initial ($\tau=0$) momentum excitation at site $m=0$.

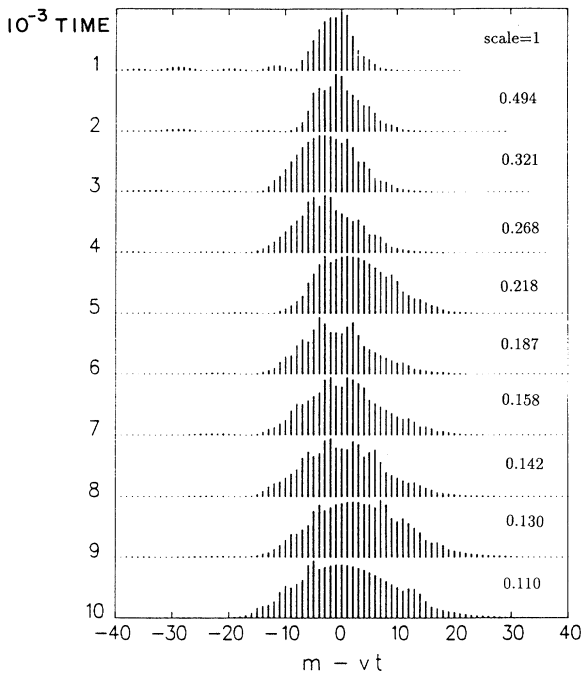

FIG. 14. Propagating peak at the sound-velocity edge in a disordered harmonic chain. Concentration $c=0.2$ of randomly distributed springs $f'/f=0.5$. The numbers on the right indicate the time decrease of the total peak energy. v: renormalized sound velocity. Initial ($\tau=0$) momentum excitation at site $m=0$.

calized and propagating parts is shown in Fig. 15. Curve 1 shows the fraction of energy stored in the propagating modes (multiplied by 5), curve 2 in localized modes, while the dotted line 3 is the first fraction multiplied by $\tau^{1/2}$. It appears that the square-root time dependence is followed rather strictly.

Since the propagating wing fronts move with a constant velocity and the energy carried by them decays as $\tau^{-1/2}$ it is clear that the second moment (7) connected with this energy contribution should behave as $\tau^{3/2}$ and the diffusion coefficient as $\tau^{1/2}$. This indeed is verified in Fig. 16. However, since these edge peaks continuously lose energy to a region behind them, this background also contributes to the diffusion coefficient. It is now remarkable that the background parts behind the propagation front give a comparable contribution to the second moment and behave in exactly the same manner (see Fig. 15), i.e., the total diffusion coefficient $D(\tau)\propto\tau^{1/2}$. The same behavior of the diffusion coefficient was found recently for an electronic system with random electron-phonon interaction [14] and called superdiffusion. The authors of Ref. [14] consider the superdiffusion as an indication of the absence of localization. It is true if one identifies the localization with the absence of diffusion. However, as we demonstrated above, the energy distribution shows all characteristic features of the usual Anderson localization. Therefore the physical situation has to be described as the coexistence of localization and superdiffusive transport.

As was pointed out in [14], the superdiffusion phenomenon is connected with three properties of the vibrational spectra: first, its boundness from below by zero frequency, second, the ω^{-2} divergence of the localization length at small frequencies, and third, the finite value of the group velocity of low-frequency (sound) waves. Due to these properties, there always exist $\sim\sqrt{N}$ modes with a mean free path of the order of the chain length spreading with a sound velocity. Therefore, using the usual definition of the diffusion coefficient $D=N^{-1}\sum_k v_k l_k$, we must take $v_k=v^*=\text{const}$, $l_k\sim N$, and restrict the sum to $\sim\sqrt{N}$ terms, which gives $D\sim\sqrt{N}$. Since in the energy propagation simulation the effective chain length is defined by the energy propagation itself, we have $N\simeq v^*\tau$, i.e., $D\sim\sqrt{\tau}$.

One can proceed beyond these qualitative arguments by using strict results concerning the eigenmodes of the disordered one-dimensional lattices [6]. In terms of eigenmodes the solution of Eqs. (4) with the initial condi-

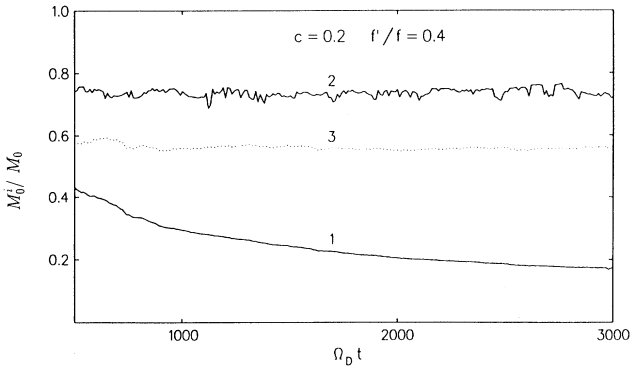

FIG. 15. Disordered harmonic chain [P excitation ($\tau=0$) at $m=0$]: time-dependent energy distribution among localized and propagating parts. c: concentration of randomly distributed springs f'. 1—energy fraction (multiplied by 5) stored in the propagating peaks at the sound-velocity edges. 2—energy stored in "localization area" $(-L,L), L=80$. 3—fraction 1 multiplied by $\sqrt{\tau}$.

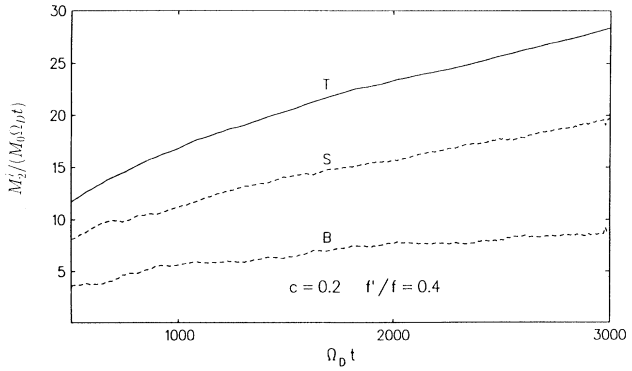

FIG. 16. Disordered harmonic chain (P excitation $\tau=0$ at $m=0$). Partial diffusion functions $D_i(\tau)=M_2^i(t)/M_0\tau$, S contribution of the sound-velocity edge peaks. B—contribution of the energy behind the sound-velocity edge; T—total. All contributions follow a $t^{1/2}$ behavior (superdiffusion).

tions (5) can be written as (see, e.g., [12])

$$P_m(\tau)=G_{m0}(\tau), \quad Q_m(\tau)=\dot{G}_{m0}(\tau) , \tag{17}$$

where

$$G_{m0}(\tau)=\sum_k \eta_m(k)\eta_0(k)\cos[(\Omega_k/\Omega_D)\tau] , \tag{18}$$

$\eta_m(k)$ being the amplitudes of the eigenmodes. The problem of the asymptotic time behavior of the Green function $G_{m0}(\tau)$ is by no means a simple one, since its Fourier transform contains N poles and the asymptotic behavior depends on the assumptions made about the contributions of different poles [15]. However, the asymptotic behavior for the case when both t and m are large is a more simple problem. We use the following property (based on the Fuerstenberg theorem on the product of random matrices) of eigenvectors in a disordered system [15]:

$$|\eta_m(k)|=|\eta_0(k)|\exp[-\lambda_k|m-m_{0k}|] \text{ for } m\to\infty , \tag{19}$$

where λ_k is the inverse localization length. Since low-frequency vibrations should be equivalent to weakly scattered phonons we can choose the eigenvectors for large $|m|$ as

$$\eta_m(k)=N^{-1/2}\exp[ikm-\lambda_k|m-m_{0k}|] . \tag{20}$$

In the limit $k\to 0$ the inverse localization length is given for our model of disorder by (up to an unimportant numerical factor)

$$\lambda_k=\lambda_0\left[\frac{\Omega_k}{\langle\Omega_D\rangle}\right]^2 , \tag{21}$$

where

$$\lambda_0=\frac{\langle(f_{m,m+1}-\langle f\rangle)^2\rangle}{\langle f\rangle^2}=\frac{c(1-c)(f'-f)^2}{[cf'+(1-c)f]^2} . \tag{22}$$

Here $\langle\Omega_D\rangle=2v^*\Omega_D$ is the maximal frequency of a mean lattice.

In terms of eigenmodes (20) we have for the Green functions

$$G_{m0}(\tau)=\sum_k \exp\{ikm-\lambda_k(|m_{0k}|+|m-m_{0k}|)\} \times\cos[(\Omega_k/\Omega_D)\tau] . \tag{23}$$

For large $|m|$ we can neglect the term containing the centers of mode localization m_{0k} because the initial excitation projection onto the modes localized far from the origin is exponentially small. Further on, due to the fast increase of λ_k we can use small-k approximations for λ_k and $\Omega_k=v^*\Omega_D k$. As a last step we replace the sum in (23) by an integral and extend the limits from $-\infty$ to ∞, which is justified by the fast decrease of the localization length. Then the result reads as

$$\langle P_m(\tau)\rangle=\frac{1}{2(\pi\lambda_0|m|)^{1/2}}\exp\left[-\frac{(|m|-v^*\tau)^2}{4\lambda_0|m|}\right] . \tag{24}$$

We observe that in the reference frame moving with average sound velocity the distribution of the averaged momenta for long times and far from the origin is approximately a diffusive one. This behavior is in a sense occasional—it is caused by the fact that the Rayleigh scattering law (21) in one dimension coincides with the diffusive pole k dependence. For large $|m|$ this pole gives the most essential contribution; other assumptions lead to a faster, at least a τ^{-1}, decay. In higher dimensions, the diffusive behavior is caused by resonant backscattering and can manifest itself only in an averaged two-particle Green function (say, in $\langle P_m^2\rangle$) but not in a one-particle function.

Using (24) and (17) we can easily show that the averaged potential and kinetic energies per atom coincide. Then the total site energy density is just given by $\langle h_m(\tau)\rangle=2\langle P_m(\tau)\rangle^2$. We observe that the time dependences for the intensity ($\propto\tau^{-1}$) and width ($\propto\tau^{1/2}$) described by this expression exactly correspond to the results of the simulation.

In the limit $v^*\tau\gg\lambda_0$ the integral intensity reads

$$\int\langle h_m(\tau)\rangle dm=\left[\frac{1}{16\pi\lambda_0 v^*\tau}\right]^{1/2} \tag{25}$$

and for the diffusion coefficient we get

$$D(\tau)=\frac{v^*}{4}\left[\frac{v^*\tau}{\lambda_0}\right]^{1/2} . \tag{26}$$

The last expression correctly describes the time dependence and the dependence on the strength of the scattering.

VI. DISORDERED ANHARMONIC LATTICE: REDUCTION OF LOCALIZATION AND INSTABILITY OF SOLITONS

Comparing Figs. 4–6 we notice that disorder on the one hand reduces the effectivity of solitonic propagation and captures some portion of the excitation energy in a bounded region near the excitation site (Anderson localization). But the localized fraction is smaller than in the purely harmonic disorder case. This is shown in Fig. 17. On the other hand, disorder has the effect of rendering the ultrasonic solitons instable. Figure 18 demonstrates this phenomenon in a moving reference frame. One observes that the soliton in the course of time returns to the sound-velocity edge and thereby it gradually loses its energy and turns broader. (In some sense it is a kind of boomerang behavior.)

As in Sec. V, we simulate harmonic disorder by a concentration c of randomly distributed springs f', whereas, as in Sec. IV, anharmonicity is represented by quartic springs in a regular array. In the continuum limit (weak anharmonicity) Ilzuka, Nakao, and Wadati [26], have given the fractional power law t^{-1} for the decay of the soliton amplitude. Our numerical results roughly confirm this behavior up to $\gamma_4\approx 0.5$ (see Fig. 19). Beyond this value the amplitude decay is still given by a power

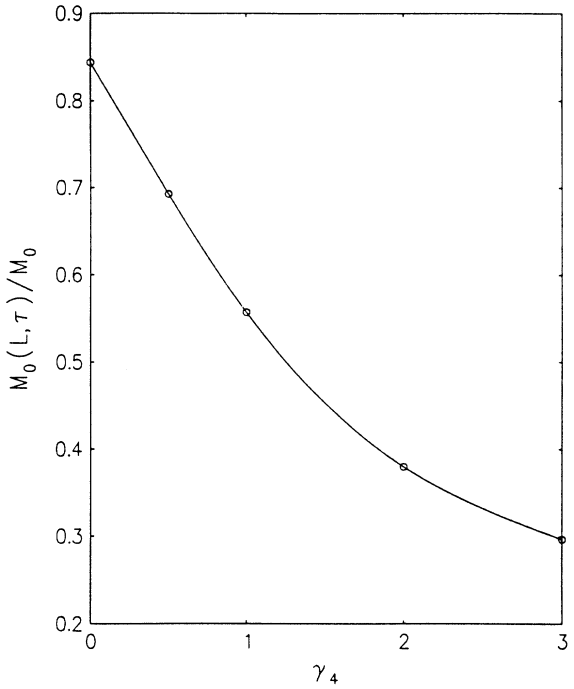

FIG. 17. Disordered anharmonic chain. Decrease of localization by anharmonicity. Change of the energy confined within the localization length L with nonlinearity parameter γ_4. $f'/f=0.5$, $c=0.2$, $L=100$. Initial ($\tau=0$) momentum excitation at site $m=0$.

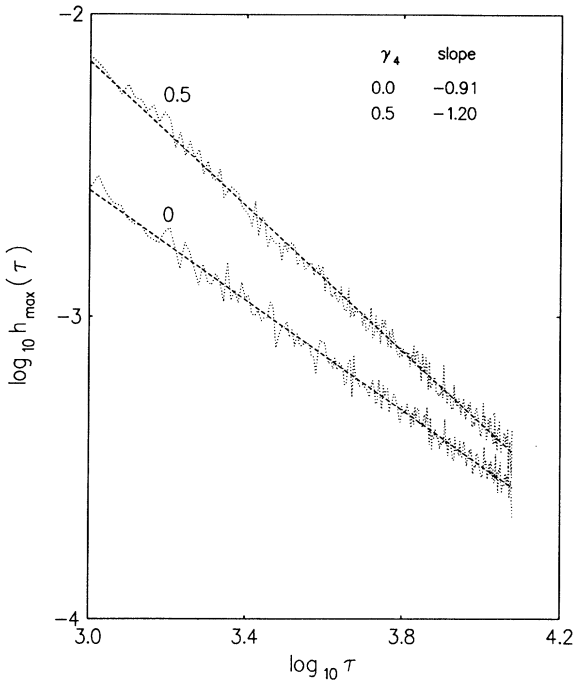

FIG. 19. Decay of the soliton amplitude in a harmonically spring disordered ($c=0.2$, $f'/f=0.5$) chain with weak anharmonicity (Wadati behavior). Initial ($\tau=0$) momentum excitation at site $m=0$.

law $t^{-\alpha}$, but α now lies above the Wadati result (see Fig. 20).

From Fig. 6 we observe that the envelope of the spatial energy distribution does not approach a shape which one could describe as a phenomenological "diffusive structure," i.e., no Gaussian shape. This is true for all considered cases of anharmonicity parameters. Nevertheless,

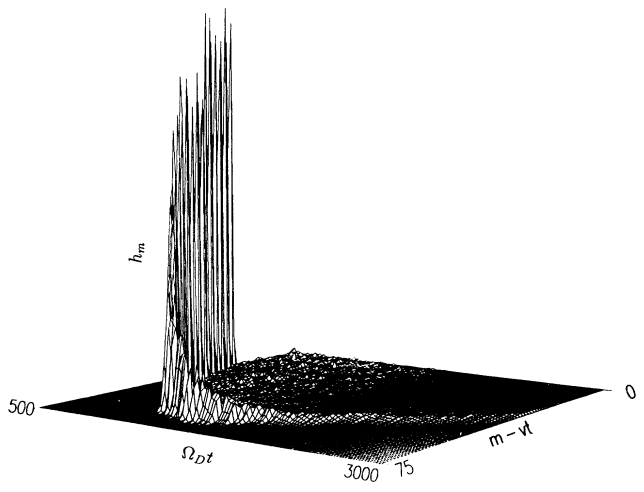

FIG. 18. Soliton propagation and decay in a moving reference frame (v is the sound velocity). Anharmonic disturbed chain [harmonic spring disorder ($c=0.2$, $f'/f=0.5$) and regular array of nearest-neighbor quartic springs].

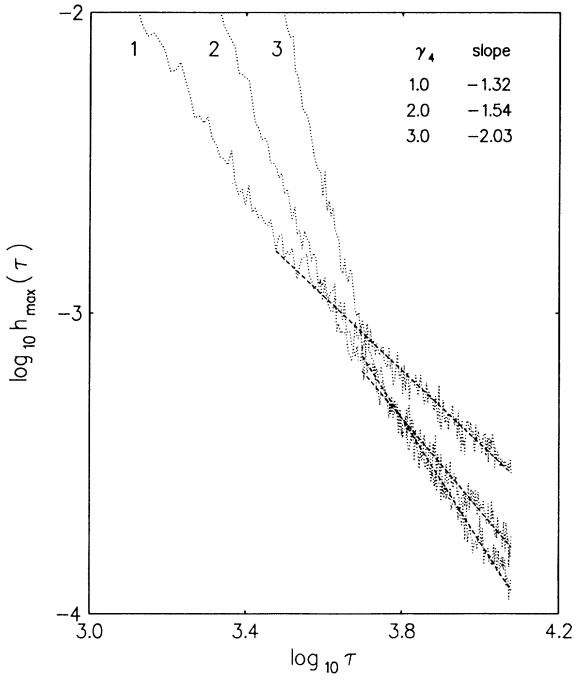

FIG. 20. Decay of the soliton amplitude in a harmonically spring disordered chain ($c=0.2$, $f'/f=0.5$) with strong quartic anharmonicity (non-Wadati behavior). Initial ($\tau=0$) momentum excitation at site $m=0$.

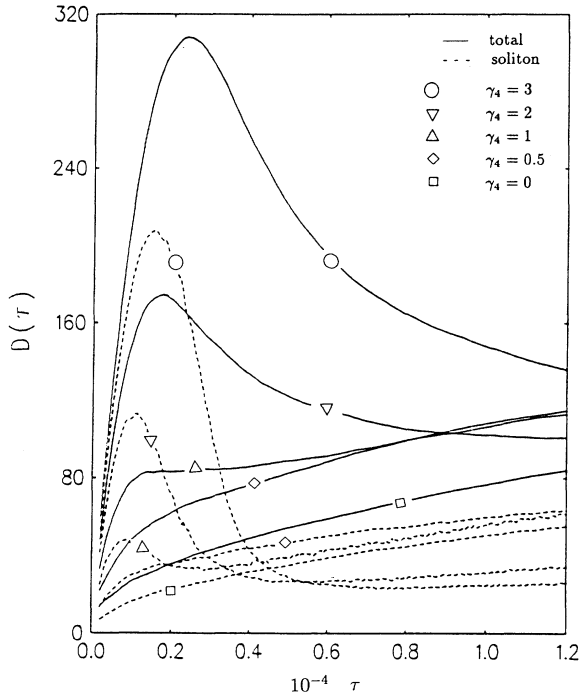

FIG. 21. Diffusion function $D(\tau)$ for different values of γ_4 (disorder parameters $f'/f=0.5$, $c=0.2$). Initial excitation at side $m=0$ ($\tau=0$).

we may formally define a diffusion function $D(\tau)=M_2(\tau)/\tau M_0$ in the same way as done in the previous sections [videlicet, Eq. (8)]. The time behavior of this quantity is given in Fig. 21 for several values of the anharmonicity parameter γ_4 and fixed disorder parameter f'/f and c. Figure 21 also shows the solitonic contribution to the diffusion function $D(\tau)$. In the degenerated case $\gamma_4=0$, i.e., the harmonic case, the contribution of the outermost peaks is taken. From the figure we note that for weak anharmonicity a superdiffusive behavior is generated, while for strong anharmonicity it seems that $D(\tau)$ approaches a constant value in the long-time regime.

VII. SUMMARY

In the present work we have investigated, mainly by exact numerical calculation, the energy propagation in a one-dimensional infinite chain, which develops after an initial impulse excitation ($p_0=M\Omega_D A$) of a single mass at site $m=0$. Within the chain nearest-neighbor interaction and equal masses of the particles has been assumed and four archetypical interaction setups have been considered: (a) a uniform array of harmonic springs (f_2), (b) a uniform array of combined harmonic (f_2) and quartic springs (f_4), (c) a randomized distribution of two different types of harmonic springs (harmonic disorder), and (d) a combination of harmonic disorder and quartic springs in a regular display.

The following dominant features have been found.

(1) In the ordered harmonic chain a sharp peak appears at the sound-velocity edges of the energy distribution, the maximal height of which decays like $\tau^{-2/3}$ in time. This behavior can also be verified analytically.

(2) If anharmonicity is added in the regular harmonic chain the wing peaks are enhanced and the inverse τ power law of their decay is reduced. Finally at $(A^2 f_4/f_2)\simeq 0.8$ they are transmuted into hypersonic solitons, which separate from the sound-velocity edges. These solitons are of compressive nature and display kink form for the particle displacement distribution $\{Q_m\}$ and a symmetrically peaked form both for the particle momenta $\{P_m\}$ and the site energies $\{h_m\}$. The maximal amplitude of P_m behaves linearly with (f_4/f_2) for weak anharmonicity and as $(f_4/f_2)^{1/2}$ for strong anharmonicity. The soliton velocity grows linearly with (f_4/f_2) both in the weak and strong coupling situations, but with different prefactors. For growing values of (f_4/f_2) new solitons are created successively, which alternately are of compressive and rarefective nature. The first rarefactive soliton appears at $(A^2 f_4/f_2)\simeq 4.8$. In the limit of a pure anharmonic lattice ($f_2=0$) the velocities of the successive solitons are related as $1:1/\sqrt{2}:1/\sqrt{6}:\cdots$ and their amplitudes are proportional to v_s^2.

(3) In the uniform anharmonic chain the second moment $M_2(\tau)$ of the energy packet strictly follows a τ^2 law, the prefactor being proportional to the energy stored in the solitons. This shows that the spatial evolution is *strictly coherent* not only for the solitary part, but also for the subsonic parts behind the solitons. Even for strong nonlinearity the transport remains *nondiffusive* ($D\sim M_2/\tau$). We have also found such behavior in a 2D anharmonic lattice.

(4) In a disordered harmonic 1D lattice the energy packet rather shortly after the time of the initial impulse separated into two components: a nonpropagating one, localized around the excitation site *(Anderson localization)* and two sharp maxima at the sound-velocity edges, which move with an average sound velocity $v^*=v[(1-c)+cf'/f]^{1/2}$, where c is the concentration of the springs f'. The maximal energy density of the edge peaks decays as τ^{-1}, and the energy stored in them declines as $\tau^{-1/2}$; thus their contribution to the second moment behaves as $\tau^{3/2}$. But also the region behind the edges contributes to the second moment. It is remarkable that this contribution to M_2 also follows a $\tau^{3/2}$ law. Hence the diffusion function behaves as $D\sim M_2/\tau\sim\tau^{1/2}$. Such behavior also has been found in disordered electronic systems and called *superdiffusion.* Thus we have found a coexistence of Anderson localization and superdiffusive transport. We have also given an analytical foundation of this phenomenon by making use of the Fuerstenberg theorem.

(5) In a disordered anharmonic lattice the main features are the *opposing tendencies* of disorder and anharmonicity: anharmonicity reduces localization, whereas disorder destroys solitonic stability. The fraction of energy captured in the neighborhood of the excitation site is smaller than in the pure harmonic case. On the other hand, disorder renders the ultrasonic solitons unstable and gradually diminishes their velocity such that the solitonic peak is getting smaller and broader and eventually returns to the sound-velocity edge. For the

decay of the solitonic amplitude Wadati has derived a τ^{-1} law in the continuum limit. Our numerical results roughly confirm this behavior up to $(A^2 f_4/f_2) \simeq 0.5$ (weak anharmonicity). Beyond this value the decay is still given by a power law $\tau^{-\alpha}$, but α now lies *above the Wadati law.* Another dominant feature of our numerical simulation is the observation that the envelope of the energy distribution never approaches a shape which one could consider as a phenomenological diffusive structure, i.e., a Gaussian shape. If a diffusive function $D(\tau)=M_2(\tau)/\tau M_0$ is introduced again, we note that for strong anharmonicity $D(\tau)$ seems to approach a constant value.

Physically the most interesting result of this work presumably is the observation that for the chosen type of initial condition (single-site impulse excitation) disorder and anharmonicity display an antagonistic tendency with respect to energy transport: while anharmonicity enforces energy propagation (ultrasonic soliton), disorder has a diminishing effect (Anderson localization). By contrast, in a forthcoming paper, in which the analogous investigation steps will be performed for another prototype of initial condition (single-site displacement excitation), it will be shown that disorder and anharmonicity both reveal the same tendency with respect to energy transport: anharmonicity captures energy in the form of standing or subsonic solitons, and disorder produces an Anderson localization which is even stronger than in the momentum excitation case.

ACKNOWLEDGMENT

One of us (G.S.Z.) wants to thank the Max Planck Institut für Festkörperforschung in Stuttgart and the Hereaus Stiftung for their financial support.

*Permanent address: Institute of Physics, Estonian Academy of Sciences, Riia 142, EE 2400 Tartu, Estonia.

[1] P. W. Anderson, Phys. Rev. **109**, 1492 (1958).
[2] K. Ishii, Suppl. Prog. Theor. Phys. Jpn. **53**, 77 (1977).
[3] S. John, H. Sompolinsky, and M. J. Stephen, Phys. Rev. B **27**, 5592 (1983).
[4] R. Orbach, Philos. Mag. B **65**, 289 (1992).
[5] W. M. Visscher, in *Vibrational Properties of Solids,* edited by G. Gilat, Methods in Computational Physics Vol. 15 (Academic, New York, 1986), p. 371.
[6] H. Matsuda and K. Ishii, Suppl. Prog. Theor. Phys. **45**, 56 (1968).
[7] T. Rolfe, S. A. Rice, and J. Dancz, J. Chem. Phys. **70**, 26 (1979).
[8] M. Toda, *Theory of Nonlinear Lattices,* Springer Series in Solid-State Sciences Vol. 20 (Springer, Berlin, 1981).
[9] Q. Li, St. Pnevmatikos, E. N. Economou, and C. M. Soukoulis, Phys. Rev. B **37**, 3534 (1988).
[10] E. Fermi, J. R. Pasta, and S. M. Ulam, Los Alamos Report No. LA-1940 (1955), published in *Collected Papers of Enrico Fermi* (University of Chicago Press, Chicago, 1965), Vol. II, p. 978.
[11] N. J. Zabusky and M. D. Kruskal, Phys. Rev. Lett. **15**, 240 (1965).
[12] M. Wagner, A. Lütze, G. Viliani, W. Frizzera, and O. Pilla, Physica B (to be published).
[13] M. Wagner, G. Zavt, J. Vazquez-Marquez, A. Lütze, Th. Mougios, G. Viliani, W. Frizzera, O. Pilla, and M. Montagna, Philos. Mag. B **65**, 273 (1992).
[14] D. Dunlap, K. Kundu, and P. Phillips, Phys. Rev. B **40**, 10 999 (1989).
[15] A. A. Maradudin, E. W. Montroll, G. H. Weiss, and I. P. Ipatova, *Theory of Lattice Dynamics in the Harmonic Approximation,* 2nd ed. (Academic, New York, 1971).
[16] W. R. Hamilton, Proc. R. Irish Acad. **267**, 341 (1839).
[17] J. Vazquez-Marquez, M. Wagner, M. Montagna, O. Pilla, and G. Viliani, Physica B **172**, 355 (1991).
[18] A. J. Sievers and S. Takeno, Phys. Rev. Lett. **61**, 970 (1988).
[19] J. B. Page, Phys. Rev. B **41**, 7835 (1990).
[20] S. E. Trullinger, V. E. Zakharov, and V. L. Pokrovsky, *Solitons,* Modern Problems in Condensed Matter Sciences Vol. 20 (North-Holland, Amsterdam, 1986).
[21] A. R. Bishop, J. A. Krumhansl, and S. E. Trullinger, Physica D **1**, 1 (1980).
[22] M. Wadati, J. Phys. Soc. Jpn. **38**, 673 (1975).
[23] M. Peyrard, St. Pnevmatikos, and N. Flytzanis, Physica D **19**, 268 (1986).
[24] R. Bourbonnais and R. Maynard, Phys. Rev. Lett. **64**, 1397 (1990).
[25] R. Livi, M. Pettini, S. Ruffo, M. Sparpaglione, and A. Vulpiani, Phys. Rev. A **31**, 1039 (1985).
[26] T. Ilzuka, T. Nakao, and M. Wadati, J. Phys. Soc. Jpn. **60**, 4167 (1991).